

**RIGA TECHNICAL UNIVERSITY**

Faculty of Mechanical Engineering, Transport and Aeronautics  
Institute of Biomedical Engineering and Nanotechnologies

**Maksims Šneiders**

Doctoral Student of the Study Programme  
“Engineering Technology, Mechanics and Mechanical Engineering”

**METHOD FOR THE DETERMINATION OF  
ACETONE VAPOUR CONCENTRATION BY  
OPTICAL STIMULATION OF THE P-N JUNCTION**

**Summary of the Doctoral Thesis**

Scientific supervisor  
Professor Dr. habil. phys.  
JURIJS DEHTJARS

RTU Press  
Riga 2022

Šneiders M. Method for the Determination of Acetone Vapour Concentration by Optical Stimulation of the p-n Junction. Summary of the Doctoral Thesis. – Riga: RTU Press, 2022. – 28 p.

Published in accordance with the decision of the Promotion Council “RTU P-16” of 12 April 2022, Minutes No. 2.

Cover design by Maksims Šneiders

<https://doi.org/10.7250/9789934227905>  
ISBN 978-9934-22-790-5 (pdf)

## ACKNOWLEDGEMENTS

I would like to express my gratitude to the supervisor of my dissertation, Professor Jurijs Dehtjars, for valuable and comprehensive advice and guidance throughout the work. Without your vision and ideas for the future, the work would not be possible.

I would like to thank my colleagues from the Institute of Biomedical Engineering and Nanotechnology for their support and ideas, which undoubtedly helped me in the implementation of the study.

Many thanks to my student, Maksims Komars, for designing the vapour delivery device prototype, obtaining experimental data and never-ending enthusiasm.

Many thanks to Fjodors Tjuļkins, Sabīne Teifurova and the Komars family for editing the paper and critical remarks.

I would especially like to express my gratitude to LLC INLAB and its manager, Maksims Poļakovs, for providing high-precision measuring equipment.

Thanks to Natālija Mozga, Secretary of the RTU P-16 Promotion Council, for consultations on design and submission of the paper.

Thanks to RTU PhD Department.

Many thanks to my friends, wife and family, especially to my grandfather Arkādijs Šneiders, who constantly supported and motivated me throughout writing of my dissertation.

**DOCTORAL THESIS PROPOSED TO RIGA TECHNICAL  
UNIVERSITY FOR THE PROMOTION TO THE SCIENTIFIC  
DEGREE OF DOCTOR OF SCIENCE**

To be granted the scientific degree of Doctor of Science (Ph. D.), the present Doctoral Thesis has been submitted for the defence at the open meeting of RTU Promotion Council on 1 July 2022, 10:00 at the Faculty of Mechanical Engineering, Transport and Aeronautics of Riga Technical University, 6B Ķīpsalas Street, Room 417.

**OFFICIAL REVIEWERS**

Professor Dr. habil. phys. Jānis Spīgulis  
University of Latvia

Dr. phys. Dmitrijs Bočarovs  
University of Latvia

Professor Dr. Arzum Erdem  
Ege University, Turkey

**DECLARATION OF ACADEMIC INTEGRITY**

I hereby declare that the Doctoral Thesis submitted for the review to Riga Technical University for the promotion to the scientific degree of Doctor of Science (Ph. D.) is my own. I confirm that this Doctoral Thesis had not been submitted to any other university for the promotion to a scientific degree.

Maksims Šneiders, .....

Date: .....

The Doctoral Thesis has been written in Latvian. It consists of Introduction, 7 chapters, Conclusions, Recommendations, 40 figures, 7 tables, 1 appendix; the total number of pages is 60, including appendix. The Bibliography contains 82 titles.

## ABBREVIATIONS AND TERMS USED IN THE WORK

Abbreviation	Explanation
$\beta$	current amplification factor
$r$	relative humidity
$t$	ambient air temperature
$v$	confidence probability
$\Delta I$	increase in output current
$\Delta \tau$	time interval of the increase in output current
$K$	vapour concentration
$U$	voltage of the electric circuit
$\Phi$	intensity of optical radiation
<b>AVID</b>	injection device for concentration of certain acetone vapour
<b>VOC</b>	volatile organic compound
<b>HgXe</b>	mercury-xenon (lamp)
<b>LED</b>	light-emitting diode
<b>MOP</b>	metal-oxide-semiconductor
<b>ppm</b>	parts per million
<b>UV</b>	ultraviolet (radiation)

# TABLE OF CONTENTS

GENERAL DESCRIPTION OF THE DOCTORAL THESIS .....	7
1. LITERATURE REVIEW.....	12
1.1. Methods of gas and vapour detection.....	12
2. PHYSICAL PRECONDITIONS FOR USING OPTICAL STIMULATION OF P-N JUNCTION .....	12
3. METHODOLOGY AND TOOLS .....	13
3.1. Vapour delivery device .....	14
3.2. Research methodology .....	16
3.2.1. Recording and processing of sensor output current.....	16
3.2.2. Connecting the sensor.....	18
4. DETERMINATION OF SENSOR OPERATING MODES AND PARAMETERS .....	18
4.1. Optical stimulation .....	18
4.1.1. Light intensity.....	18
4.1.2. Spectral band .....	18
4.2. Electrical circuit voltage.....	19
4.3. Optical surface degassing.....	19
4.4. Current amplification factor .....	19
5. DETERMINATION OF THE ACETONE VAPOUR CONCENTRATION THRESHOLD ...	19
5.1. Without degassing and with low current amplification factor .....	19
5.2. With degassing and high current amplification factor .....	20
6. METHOD FOR THE DETERMINATION OF ACETONE VAPOUR CONCENTRATION USING A SENSOR BASED ON OPTICAL STIMULATION OF A P-N JUNCTION .....	21
6.1. Comparison of the method with available analogues worldwide.....	21
6.2. Procedure for the use of the acetone vapour concentration method.....	22
7. RECOMMENDATIONS. POSSIBILITIES OF USING THE METHOD .....	24
CONCLUSIONS .....	25
BIBLIOGRAPHY .....	27

## GENERAL DESCRIPTION OF THE DOCTORAL THESIS

### Topicality

Acetone is one of the ketones and is metabolised by liver, while acetone vapour is a volatile organic compound (VOC) that has been identified as a biomarker. Based on several studies, acetone levels outside the specified range may indicate a metabolic disease [1]–[4].

Acetone vapour is produced in various concentrations in the production and storage of consumer goods, commercial goods, construction materials, etc. Elevated acetone vapour concentrations can adversely affect working conditions and the environment, so determination of acetone vapour concentrations is required [5]–[7].

In the range of modern sensors, semiconductor structures are best suited for determining VOC concentrations. These sensors are compact devices suitable for detecting low vapour concentrations [8]–[10], however, this type of sensor has a drawback – its operation requires maintaining the sensitive part of the sensor (the part of the sensor whose electrical properties change in the presence of the target gas/vapour) at high temperatures. To prevent this, in recent years, semiconductor sensors have been stimulated with UV radiation, which changes the concentration of charge carriers in the semiconductor on which the gas/vapour molecules are absorbed and as a result the current of the sensor output. This current depends on the amount of gas/vapour molecules absorbed. With such sensors, the concentration of acetone vapour can be measured without heating the sensitive part of the sensor, but this method has a relatively high detection threshold, which makes it difficult to determinate VOCs in the patient's exhalation in cases of gastrointestinal diseases, diabetes or other pathologies.

The sensitivity of the sensor can be increased by using an exponential relationship between the number of molecules absorbed and the photogenerated current through the p-n junction of the semiconductor device.

The Thesis is devoted to the development of a method for the detection of low concentrations of acetone vapour (less than 100 ppm) and the design of a suitable sensor using optical stimulation of p-n junction without heating the sensing part of the sensor.

As a result of the Thesis, a method for determination of acetone vapour concentration using a novel p-n junction optically stimulated sensor was implemented, allowing to determine acetone vapour concentration in the range from 16.3 ppm to 13 060 ppm (relative to a 1 mm<sup>2</sup> sensitive part from 0.636 ppm to 509 ppm) in air.

### The aim of the Thesis

To develop a method for the determination of acetone vapour concentration using a novel sensor based on optical stimulation of the p-n junction.

### **The following tasks were set to achieve the goal of the Thesis:**

1. Rationale for a method which provides a variation of the photogenerated output current with the concentration of acetone vapour in air.
2. Sensor development based on a substantiated method.
3. Development of a study methodology and a vapour delivery apparatus for the time-resolved recording of the sensor current versus acetone vapour concentration in air.
4. Investigation of the operating modes of the sensor and determination of the associated parameters:
  - optical stimulation mode;
  - voltage of the electrical circuit;
  - optical degassing of the surface;
  - current amplification factor.
5. Determination of the time interval between the increase of the sensor current and the increase of the sensor current as a function of the concentration of acetone vapour in air.
6. Implementation of the method for the determination of acetone vapour concentration in air using the new p-n junction based optically stimulated sensor. Method application procedure.
7. Possibilities of using the method: system size reduction, system operability outside standard conditions, selective sensor concept.

### **Theses for defence**

1. A method for the determination of acetone vapour concentration in air is developed with a new sensor in which the p-n junction, a bipolar germanium alloy, is optically stimulated (HgXe lamp radiation, light flux  $\Phi = 4.65 \text{ mW/cm}^2$ ).
2. The sensor operates over a concentration range of 16.3 ppm to 13 060 ppm of acetone vapour.
3. The emitter current of a p-n junction-based optically stimulated sensor depends exponentially on the concentration of acetone vapour in air.
4. The detection threshold for acetone vapour is 0.636 ppm (per  $1 \text{ mm}^2$  of sensing area) using the following operating mode parameters: HgXe lamp;  $\Phi = 4.65 \text{ mW/cm}^2$ ;  $\Phi_{\text{degassing}} = 77.5 \text{ mW/cm}^2$ ;  $U = 12 \text{ V}$ ;  $\beta = 152$ ; coupling circuit – emitter repeater with common base, ambient conditions:  $t = 20 \pm 1 \text{ }^\circ\text{C}$ ;  $r = 45 \pm 5 \%$ .
5. A new method for the determination of acetone vapour concentration using a sensor based on optical stimulation of the p-n junction allows to determine a minimum concentration of acetone vapour in air of 0.636 ppm (relative to a sensing area of  $1 \text{ mm}^2$ ) with an uncertainty of 2.0 % (95 % confidence probability).

### **Scientific novelty of the Thesis**

1. A method for the determination of acetone vapour concentration in air has been implemented, which by optical stimulation of a sensor on a p-n junction provides measurements of acetone



- concentration in the range of 16.3 ppm to 13 060 ppm with an uncertainty of 2.0 % (95 % confidence probability;  $t = 20 \pm 1$  °C;  $r = 45 \pm 5$  %) by measuring the increase in output current.
2. It has been shown that by measuring the time interval of the increase in output current of a sensor on a p-n junction under optical stimulation, it is possible to measure acetone concentrations between 16.3 ppm and 13 060 ppm with an uncertainty of 11 s (95 % confidence probability;  $t = 20 \pm 1$  °C;  $r = 45 \pm 5$  %).
  3. The emitter current of a p-n junction-based optically stimulated sensor has been shown to depend exponentially on the concentration of acetone vapour in air. A sensor based on optical stimulation of the p-n junction, which does not need to be heated, has been developed to detect the concentration of acetone vapour in air. The lower threshold for the detection of acetone is 0.636 ppm, and the upper threshold is 509 ppm per 1 mm<sup>2</sup> of sensing area. The minimum detectable concentration is 79 times lower compared to the concentration detection methods using optically stimulated sensors currently available on the market.

### **Practical significance of the Thesis**

A method for the detection of acetone vapour concentration using a p-n junction based optical stimulation sensor that can be used to detect acetone vapour concentrations in air up to a threshold of 0.636 ppm (relative to a sensing area of 1 mm<sup>2</sup>) has been developed. The method can be used for medical (biomarker detection), occupational, environmental and anti-terrorism purposes.

### **Approbation of the Thesis**

The results of the Thesis were presented at the following conferences:

1. 9th International Conference On BIONICS and PROSTHETICS BIOMECHANICS and MECHANICS MECHATRONICS and ROBOTICS, 17–21 June 2013, Riga, Latvia.
2. 54th International Scientific Conference of Riga Technical University, 14–16 October 2013, Riga, Latvia.
3. 55th Student Scientific Technical Conference of Riga Technical University, 29 April 2014, Riga, Latvia.
4. 1st European Biomedical Engineering Conference for Young Investigators, 28–30 May 2015, Budapest, Hungary.
5. 56th International Scientific Conference of Riga Technical University, 14–16 October 2015, Riga, Latvia.
6. XIV Mediterranean Conference on Medical and Biological Engineering and Computing, 31 March – 2 April 2016, Pathos, Cyprus.
7. 57th International Scientific Conference of Riga Technical University, 14–18 October 2016, Riga, Latvia.
8. The joint conference of the European Medical and Biological Engineering Conference (EMBEC) and the Nordic-Baltic Conference on Biomedical Engineering and Medical Physics (NBC), 11–15 June 2017, Tampere, Finland.

9. World Congress on Medical Physics & Biomedical Engineering, 3–8 June 2018, Prague, Czech Republic.
10. 59th International Scientific Conference of Riga Technical University, 10–12 October 2018, Riga, Latvia.
11. XV Mediterranean Conference on Medical and Biological Engineering and Computing, September 26–28, 2019, Coimbra, Portugal.

### **Publications**

#### Scientific publications and contribution by the author of the Thesis:

1. Dekhtyar, Y., Komars, M., Sneiders, M., Selutina, M. Towards Optically Induced Semiconductor Gas Sensor: Sensing of Acetone. IFMBE Proceedings, 2015, 50, 63–65. Available from: doi:10.1007/978-981-287-573-0 (**SCOPUS**)  
*M. Šneiders' contribution: research method, experiments, writing the publication.*
2. Dekhtyar, Y., Selutina, M., Sneiders, M., Zunda, U. Towards Optically Induced Semiconductor Human Exhalation Gas Sensor. IFMBE Proceedings, 2016, 57, 482–485. Available from: doi:10.1007/978-3-319-32703-7 (**SCOPUS**)  
*M. Šneiders' contribution: research method, experiments, writing the publication.*
3. Dekhtyar, Y., Komars, M., Morozovs, F., Sneiders, M. Optically Induced Semiconductor Gas Sensor: Acetone Detection Range using Continuous and Cyclic Optical Irradiation Types. IFMBE Proceedings, 2018, 65, 330–333. Available from: doi:10.1007/978-981-10-5122-7 (**SCOPUS**)  
*M. Šneiders' contribution: research method, experiments, writing the publication.*
4. Dekhtyar, Y., Komars, M., Sneiders, M. Semiconductor Ethanol Sensor Inducted with Visible Light. IFMBE Proceedings, 2019, 68/3, 3–6. Available from: doi:10.1007/978-981-10-9023-3 (**SCOPUS**)  
*M. Šneiders' contribution: research method, experiments, writing the publication.*
5. Dekhtyar, Y., Komars, M., Sneiders, M. Optical Metrology of Novel Optically Stimulated Semiconductor Gas Sensor. IFMBE Proceedings, 2020, 76, 462–468. Available from: doi:10.1007/978-3-030-31635-8 (**SCOPUS**)  
*M. Šneiders' contribution: research method, experiments, writing the publication.*

#### Patent

1. RIGAS TEHNISKĀ UNIVERSITĀTE. *Gāzes detektēšanas sensors, izmantojot diožu optisko stimulāciju*. Jurijs Dehtjars, Maksims Komars, Maksims Šneiders (inventors). Int. Cl.: G01N 21/33; G01N 21/59; H01L 21/02; H01L 23/20; H01L 23/467. Date of submission 2020-12-18. LV 15569 B1. Publication on 2021-10-20.  
*M. Šneiders' contribution: research method, experiments, writing the patent.*

### Conference abstracts

1. Dehtjars, J., Šneiders, M. Towards Optically Stimulated Semiconductor for Gas Sensing. In: *The 9th Baltic-Bulgarian Conference on Bionics and Prosthetics, Biomechanics and Mechanics, Mechatronics and Robotics (ICBBM 2013): Proceedings*, Latvia, Riga, 17–18 June 2013. Riga: ICBBM Conference Committee, 2013, pp. 219–220. ISBN 978-9934-8409-0-6.
2. Dehtjars, J., Šneiders, M. Ethanol and Isopropanol Sensing Possibility Using Optically Stimulated Semiconductor. In: *RTU 55th Student Scientific Technical Conference*, Latvia, Riga, 29 April 2014. Riga: RTU, 2014, pp. 1–3.
3. Komars, M., Šneiders, M. Optically Stimulated Semiconductor Gas Sensitivity Dependence on Its Conductivity Type. In: *RTU 55th Student Scientific Technical Conference*, Latvia, Riga, 29 April 2014. Riga: RTU, 2014, pp. 1–3.
4. Dekhtyar, Y., Komars, M., Sneiders, M., Selutina, M. Towards Optically Induced Semiconductor Gas Sensor: Sensing of Acetone. In: *First European Biomedical Engineering Conference for Young Investigators*, Hungary, Budapest, May 28–30 2015. p. 20.
5. Dekhtyar, Y., Komars, M., Morozovs, F., Sneiders, M. Optically Induced Semiconductor Gas Sensor: Acetone Detection Range using Continuous and Cyclic Optical Irradiation Types. In: *Abstract book at EMBEC'17 & NBC'17*, Finland, Tampere, June 11–15, 2017. p. 304.
6. Dekhtyar, Y., Komars, M., Sneiders, M. Semiconductor Ethanol Sensor Inducted with Visible Light. In: *World Congress on Medical Physics and Biomedical Engineering: Book of Abstracts*, Czech Republic, Prague, June 3–8, 2018. Prague, 2018, p. 676.

# 1. LITERATURE REVIEW

## 1.1. Methods of gas and vapour detection

There are different methods for detecting and analysing a wide range of VOCs. They are implemented using sensors that work on different principles [11]–[14]. Within the range of modern methods for detecting acetone vapour concentrations, sensors based on semiconductor structures are best suited for detecting low vapour concentrations. This method has the additional advantage of lower energy consumption and smaller sensor dimensions (Table 1.1).

Table 1.1

Comparison of Gas/Vapour Detection Methods [8], [9]

Parameter	Gas/vapour detection method				
	semiconductor	catalytic combustion	electro-chemical	thermal conductive	infrared absorption
Sensitivity	excellent	good	excellent	bad	excellent
Accuracy	good	excellent	good	good	excellent
Selectivity	poor	bad	good	bad	excellent
Response time	excellent	good	poor	good	good
Stability	excellent	good	bad	good	good
Maintenance	excellent	good	bad	good	poor
Cost	excellent	excellent	good	good	poor
Concentration	few ppm	from 10 ppm	1–1000 ppm	1–100 %	1 ppm–100 %

Compared to the previous group of sensors (see Sections 1.2 and 1.3 of the Thesis), a sensor capable of detecting low concentrations of acetone vapour must be developed. One of the possible solutions is to create a sensor for which the current value changes non-linearly depending on the vapour concentration – an increase in the vapour concentration causes an exponential increase in the current value. The nonlinear relationship can be achieved by providing a tunnelling effect. Based on the literature review, tasks were set to achieve the goal (see Chapter General Description of the Thesis).

## 2. PHYSICAL PRECONDITIONS FOR USING OPTICAL STIMULATION OF P-N JUNCTION

Polarized gas/vapour molecules, upon contact with the surface of a semiconductor, change the concentration of free charge carriers in the leading layer of the semiconductor (Debye length). Assuming that the charge of the adsorbed molecules is evenly distributed over the surface, an equivalent charge with the opposite sign appears in the semiconductor layer. As a result, the energy

zones bend in the semiconductor layer. The depth of interaction of the adsorbed molecules in the semiconductor is limited by the depth of the Debye length.

When the semiconductor is irradiated, electron/hole pairs are generated, which shift the Fermi level towards the centre of the semiconductor restricted energy zone. In this case, the probability for electron  $f(E)$  to reach a level with energy  $E$  is subject to the Fermi-Dirac distribution function [15]. The distribution function has two parameters: Fermi level and temperature.

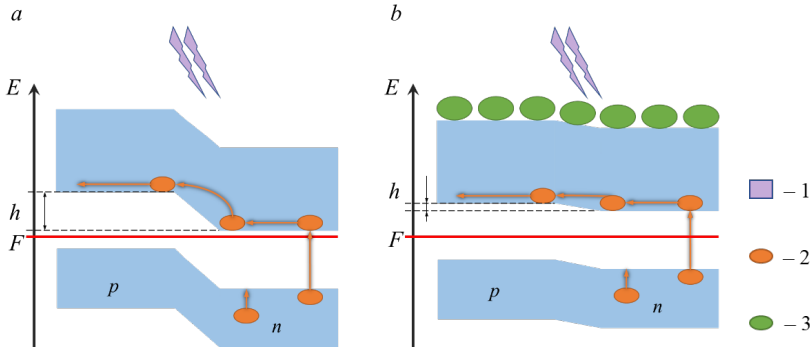


Fig. 2.1. Overcoming the electron p-n junction potential barrier: a – at optical stimulation; b – at additionally adsorbed polarized molecules.  
 Symbols: 1 – optical stimulation; 2 – free charge carriers;  
 3 – test gas/vapour molecules; F – Fermi level; h – p-n junction potential barrier height.

Adsorption of a polarized molecule causes changes in the height of the p-n junction potential barrier (Fig. 2.1), which changes the probability of photogenerated electrons to cross the p-n junction potential barrier. In the light of the above, it is possible to design a method based on an optically stimulated p-n junction and having a nonlinear (exponential) dependence of the current on the number of adsorbed molecules.

### 3. METHODOLOGY AND TOOLS

As discussed in the chapter on physical preconditions, a semiconductor with a p-n junction was required, for which optical stimulation photons can overcome the band gap in the semiconductor. The surface of the semiconductor should not be covered with a thick protective layer that could shield the interaction of the adsorbed molecule and the semiconductor, for example, for silicon semiconductors the thickness of the oxide layer ( $\text{SiO}_2$ ) can reach  $0.6 \mu\text{m}$ , which exceeds the Debye length [16]. The optical stimulation energy used had to be in the range of a few eV but higher than the average heat energy to avoid possible thermal noise.

The method of manufacturing a semiconductor without an additional protective layer is called fused technology. In order to meet the requirements described above, a fused bipolar transistor

(sensor) [17], was taken as a sensor, the construction of which includes opposite closed p-n junctions. The use of a transistor made it possible to amplify the current without developing and constructing an additional amplification circuit.

The parameters for determining the sensor's performance were: the increment in output current ( $\Delta I$ ) and the time interval of the increment in output current ( $\Delta \tau$ ). The first parameter describes the density of the adsorbed molecules, the second parameter addresses the rate of adsorption.

The studies were performed under standard conditions ( $t = 20 \pm 1$  °C;  $r = 45 \pm 5$  %), maintained in the laboratory premises of the BIN Institute.

### 3.1. Vapour delivery device

In order to achieve the goal set in the Thesis, a vapour delivery device was created.

An electrical circuit was set up to ensure the recording of the sensor emitter current (hereinafter – current). The circuit is designed as an emitter repeater with a common base. A current limiting resistor R4 was added to meet the requirements of the transistor manufacturer. It was experimentally determined that the drift of the registered current value is lower if the collector is placed in place of the emitter, and vice versa. This circuit has a high current amplification factor and high temperature stability [18].

AVID (Fig. 3.1) was formed from two cylinders with freely movable pistons. The digital caliper was used to determine the displacement of the piston, then it was converted to the volume of the injected vapour (the coefficient was checked through the weighed mass of water distillate). The acetone evaporation system consisted of an evaporation flask placed in a water bath. Using silicone tubes, shut-off valves, and t-shaped transitions, AVID was assembled in one circuit and connected to the test chamber.

In case the study had to be performed in a saturated acetone vapour environment, chemically pure acetone with a volume of  $V = 6.0$  ml (*EMSURE Acetone for analysis*) was poured into the bottom of the chamber (feed duration  $t = 5$  s). Evaporation of acetone in the chamber space provided a saturated acetone vapour environment. In this case, work with AVID was not required.

The determination of the acetone vapour concentration, which is lower than the saturated acetone vapour concentration, was based on the method of diluting the vapour mixture between the two cylinders until the desired value is reached [19].

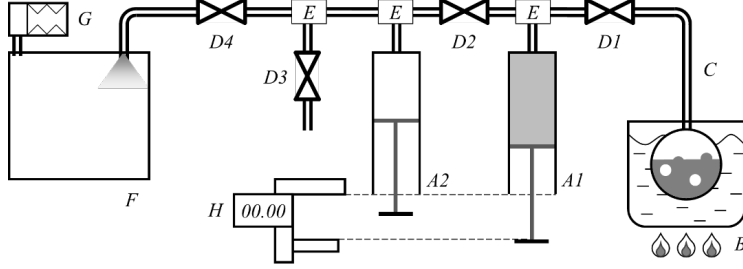


Fig. 3.1. AVID functional scheme.

Symbols: A1 – primary cylinder; A2 – secondary cylinder; B – evaporation flask in a heating bath with water; C – pipe; D1, D2 – shut-off valve; D3 – clip; E – t-type connector; F – test camera; G – pressure equalization variable volume; H – digital calliper.

First, acetone saturated vapour was prepared in cylinder A1. For this purpose, an evaporating flask filled with chemically pure acetone  $V = 2.3$  ml was immersed in a heating bath with water above the boiling point of acetone ( $t_{\text{boil}} = 56.5$  °C). The acetone was evaporated in an evaporating flask and mixed with the previously prepared volume of air in cylinder A1 forming an acetone-saturated vapour, the concentration of which was estimated using Equation (3.1) [20], [21]:

$$K_0 = \frac{P(\text{sat})}{P(\text{atm})} \cdot 10^6, \quad (3.1)$$

where  $K_0$  – concentration of saturated acetone vapour, ppm;  $P(\text{sat})$  – the pressure of saturated acetone vapour, bar; and  $P(\text{atm})$  – atmospheric pressure, bar.

The pressure of the saturated acetone vapour was calculated using the Antoine equation [22]. The deviation of the theoretical results from the experimental data using this equation was estimated to be less than 0.1% (at room temperature) [23].

$$P(\text{sat}) = 10^{\left(A - \frac{B}{T(\text{atm}) + C}\right)}, \quad (3.2)$$

where  $A$ ,  $B$ ,  $C$  are Antoine equation constants and  $T(\text{atm})$  is ambient temperature, °C.

Before proceeding, the temperature of the saturated acetone vapour in cylinder A1 was reduced to ambient temperature (monitored by measuring the surface temperature of cylinder A1 and visually observing the condensation of acetone inside cylinder A1). Subsequent steps were designed to achieve the desired vapour concentration by diluting the vapour mixture between cylinders A1 and A2 (feed volume less than diluent volume; mixture feed time  $t = 5$  s) with the prepared portion of air in the target cylinder. Each subsequent vapour concentration was estimated using Equation (3.3) [24]:

$$K(\text{new}) = K(\text{feed}) \cdot \frac{V(\text{feed})}{V(\text{air}) + V(\text{feed})}, \quad (3.3)$$

where  $K(\text{feed})$  is acetone vapour concentration in the feed cylinder, ppm;  $V(\text{feed})$  is the volume of mixture in the feed cylinder, ml; and  $V(\text{air})$  is the pre-prepared volume of air in the target cylinder, ml.

The desired concentration was obtained by varying the volume of mixture delivered and the volume of air prepared in the cylinders. Concentration calculations took into account that vapour dilution occurs when the vapour mixture is fed to the test chamber.

Maximum relative inlet acetone vapour concentration error achieved at minimum inlet acetone vapour volume using one dilution cycle:

$$\varepsilon K(\text{new}) = 2.9 \%$$

The calculated relative error value was also used for the other injected acetone vapour concentrations.

### **3.2. Research methodology**

In a series of studies on  $\Delta\tau$ , it was experimentally determined that it is reached within 180 s after the moment of acetone injection into the test chamber [25], [26], thus each stage is taken to be 180 s long. The research procedure consisted of 5 stages.

Mean values, confidence probability, standard deviations,  $\Delta I$  and  $\Delta\tau$  were calculated using *Microsoft Excel 2016 64-bit (version: 16.0.11231.20122)*.

In the study, the first three measurements were not included in the results because  $\Delta I$  and  $\Delta\tau$  are outside the confidence probability. It was experimentally determined that the next 7 measurements (4–10) were within the confidence interval.

#### **3.2.1. Recording and processing of sensor output current**

The recorded output current was experimentally determined to have zero drift (Fig. 3.2, left). The nature of zero drift is not the subject of the Thesis and was not investigated. Before the sensor current was measured, the digital multimeter data (recorded output current) was processed.



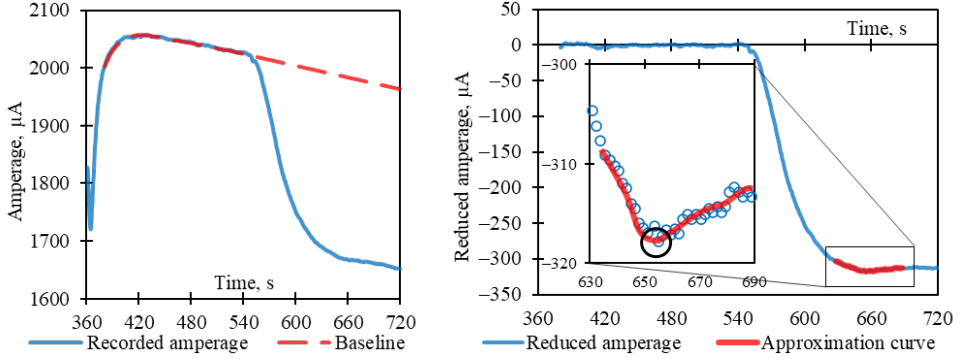


Fig. 3.2. Recorded output current with a defined baseline (left); reduced output current with overlap point (right).

Digital multimeter data were processed in OriginLab OriginPro 2018 (64-bit) SR1 (*version: b9.5.1.195*). A graph was created from the data, the baseline subtraction function (*Peak Analyzer, Goal: Subtract Baseline*) was selected in the program. A minimum of 7 points (*Baseline Mode: User Defined*) during the optical simulation period from 380 s to 535 s were selected for manual baseline (*BSpline*) detection. The time period from 360 s to 380 s was not taken into account due to uncontrolled transition processes. The reduced recorded current (Fig. 3.2 on the right) is the difference between the recorded current and the baseline.

Noise compensation of the reduced current value (Fig. 3.2 on the right) was performed with a 9th order polynomial approximation constructed for a period of  $\pm 20$  s from the transition point.

The  $\Delta I$  of the sensor is equal to the current value at the excess point (Fig. 3.2 to the right) obtained after the acetone vapour injection in relation to the recorded current value in the reference medium before the acetone vapour injection into the test chamber [19].

$$\Delta I = \frac{I(\text{ac})}{I_0} \cdot 100 \%, \quad (3.4)$$

where  $I_0$  is raw current value before acetone vapour injection,  $\mu\text{A}$ , and  $I(\text{ac})$  is the value of the reduced current at the excess point – reached after the injection of acetone,  $\mu\text{A}$ .

In addition,  $\Delta\tau$  after the moment of acetone injection into the test chamber was investigated.

$$\Delta\tau = \tau(\text{sat}) - \tau(\text{inj}), \quad (3.5)$$

where  $\tau(\text{inj})$  is the start of acetone vapour injection into the test chamber, s, and  $\tau(\text{sat})$  is the moment when the overlay point is reached in the reduced and recorded current phase, s.

### 3.2.2. Connecting the sensor

The type of connection of the sensor was studied for the efficiency of the selected electrical circuit. The results showed that with increasing concentration, the change in current  $\Delta I$  increases. Acetone vapour concentration range was 1700 ppm to 7100 ppm. The change in current  $\Delta I$  with two p-n junctions was greater than with one p-n junction.

## 4. DETERMINATION OF SENSOR OPERATING MODES AND PARAMETERS

### 4.1. Optical stimulation

#### 4.1.1. Light intensity

Continuous optical stimulation was chosen for the study [26], [27], [29].

In the results, two pronounced extremes were identified at optical radiation intensity values  $\Phi_1 = 3.10 \text{ mW/cm}^2$  and  $\Phi_2 = 15.5 \text{ mW/cm}^2$ .  $\Delta I$  changes with decreasing acetone vapour concentration, as well as at high values of optical radiation intensity.

The maximum  $\Delta\tau$  was determined when the minimum of the studied radiation intensity was equal to  $\Phi = 1.55 \text{ mW/cm}^2$ .  $\Delta\tau$  decreases with decreasing acetone vapour concentration and with increasing intensity of optical stimulation.

The maximum  $\Delta I$  was observed at the lowest optical radiation intensity  $\Phi = 1.55 \text{ mW/cm}^2$ , however, at this intensity it was not possible to determine  $\Delta\tau$ . In order to study  $\Delta\tau$ , the value of radiation intensity  $\Phi = 4.65 \text{ mW/cm}^2$  was chosen in the following studies.

#### 4.1.2. Spectral band

Analysing the results, the same  $\Delta I$  was found both at the UV radiation band and at the full (unfiltered) radiation spectrum of the HgXe lamp. Under the influence of radiation,  $\Delta I$  was the same in both the infrared and visible light spectral bands of HgXe lamps, but differed using the UV spectral band of HgXe lamps – the result was 11 times lower.

The difference in  $\Delta I$  between the full spectrum of optical stimulation radiation and the UV radiation band was not significant, therefore further studies were performed using optical stimulation without a light filter.

## 4.2. Electrical circuit voltage

The aim of the studies was to find the optimal voltage that was applied to the electrical circuit (similar to [28]). To achieve the goal, 5 separate studies with circuit voltages  $U = 3; 6; 9; 12; 15$  V were performed using DC power supply IPS-1 (*ИПС-1*).

The maximum  $\Delta I$  was found at a voltage of  $U = 15$  V. As the circuit voltage decreased,  $\Delta I$  decreased to  $U = 6$  V and began to increase at a lower voltage. As the circuit voltage decreased,  $\Delta\tau$  also decreased.

Given that  $U = 15$  V is the maximum allowable operating supply voltage and  $\Delta I$  approaches saturation, the circuit voltage was assumed to be  $U = 12$  V for further studies.

## 4.3. Optical surface degassing

The procedure of the study (see Section 3.2) was changed and an additional stage – surface optical degassing (hereinafter – degassing) was added. Degassing took place after switching on the power supply but before the start of the optical stimulation. The degassing stage was performed for 60 s at the optical stimulation intensity  $\Phi_{\text{degassing}} = 77.5$  mW/cm<sup>2</sup>. An HgXe lamp was used as the source of optical degassing. The lamp was switched off for further 20 s. The following stage of optical stimulation was performed – reduced to 100 s.

During the degassing stage, the average  $\Delta I$  increases 2.6 times. The mean  $\Delta\tau$  did not show a statistically significant deviation ( $p = 0.34$ ).

## 4.4. Current amplification factor

The variance of this coefficient was observed in the sensors. Analysing the effect of changes in the current amplification factor on the results, two transistors of the same brand with the lowest and highest found current amplification factor were taken.

Using the sensor with the highest coefficient ( $\beta = 316$  versus  $\beta = 33$ ), the mean  $\Delta I$  increased 3.4 times. The mean  $\Delta\tau$  in this case decreased 3.0 times.

# 5. DETERMINATION OF THE ACETONE VAPOUR CONCENTRATION THRESHOLD

## 5.1. Without degassing and with low current amplification factor

Figure 5.1 shows the effect of different acetone vapour concentrations on  $\Delta I$  and  $\Delta\tau$  using the following operating parameters of the sensor:  $U = 12$  V;  $\Phi = 4.65$  mW/cm<sup>2</sup>.  $\Delta I$  and  $\Delta\tau$  varied exponentially with acetone vapour concentration.

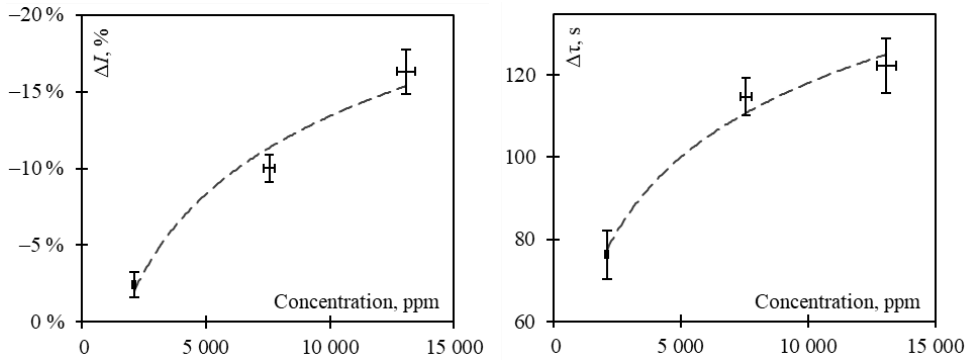


Fig. 5.1. Estimation of acetone vapour concentration using a sensor.  
Research conditions:  $\nu = 95\%$ ;  $\beta = 33$ .

The minimum  $\Delta I = -2.4\%$  was reached at an acetone vapour concentration of  $K = 2110$  ppm. When recalculating the minimum concentration value for a sensitive area of the sensor of  $1 \text{ mm}^2$ , Equation (5.1) was used to determine

$$K_{1\text{mm}^2} = \frac{S_{\text{jut}}}{1 \text{ mm}^2} \cdot K = \frac{0.0390}{1} \cdot 2110 = 82.3 \text{ ppm}, \quad (5.1)$$

where  $S_{\text{sens}}$  is the area of the sensitive part of the sensor,  $\text{mm}^2$ .

As the concentration of acetone vapour increased,  $\Delta I$  increased exponentially. When graduating from sensor  $\Delta I$ , the uncertainty did not exceed  $1.4\%$  (95% confidence probability).

As the concentration of acetone vapour increased,  $\Delta \tau$  increased exponentially. The minimum  $\Delta \tau = 76 \text{ s}$  was reached at the minimum acetone concentration value. When graduating from sensor  $\Delta \tau$ , the uncertainty did not exceed  $6.7 \text{ s}$  (95% confidence probability).

## 5.2. With degassing and high current amplification factor

The results of the same brand of transistors with increased current amplification factor and previous degassing are shown in Fig. 5.2.

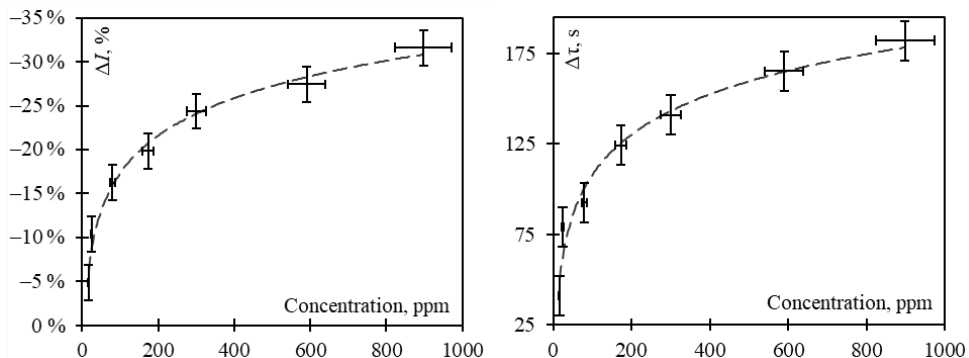


Fig. 5.2. Estimation of acetone vapour concentration using a sensor.

Research conditions:  $\nu = 95\%$ ;  $\beta = 152$ .

The minimum  $\Delta I = -4.86\%$  was reached at an acetone vapour concentration of  $K = 16.3$  ppm. By recalculating the minimum concentration value for an area of  $1 \text{ mm}^2$  of the sensitive part of the sensor, based on Expression (5.1), the following was determined:

$$K_{1\text{mm}^2} = 0.636 \text{ ppm.}$$

As the concentration of acetone vapour increased,  $\Delta I$  increased exponentially. When graduating from the  $\Delta I$  of the sensor, the uncertainty did not exceed  $2.0\%$  (95% confidence probability).

As the concentration of acetone vapour increased,  $\Delta \tau$  increased exponentially. The minimum  $\Delta \tau = 41.1 \text{ s}$  is reached at the set minimum acetone concentration. When graduating from sensor  $\Delta \tau$ , the uncertainty did not exceed  $11 \text{ s}$  (95% confidence probability).

For previously available and semiconductor-based optically stimulated sensors (see Section 1.1), the recalculated concentration threshold at an active surface area of  $1 \text{ mm}^2$  was determined based on Expression (5.1):

$$K_{1\text{mm}^2} \approx 50 \text{ ppm.}$$

## 6. METHOD FOR THE DETERMINATION OF ACETONE VAPOUR CONCENTRATION USING A SENSOR BASED ON OPTICAL STIMULATION OF A P-N JUNCTION

### 6.1. Comparison of the method with available analogues worldwide

A new method for the determination of acetone vapour concentration has been developed. The method is implemented using a sensor based on p-n junction optical stimulation. The essence of

the method is based on the development of a semiconductor vapour detection method with optical stimulation of p-n junction.

The physical conditions of the method allow the implementation of a sensor for the determination of acetone vapour concentration without the disadvantage of the semiconductor vapour detection method – heating of the sensitive part of the sensor, which is necessary for the operation of the method, and consequently no heating of the sensitive part of the sensor and diffusion of adsorbed vapour molecules into the sensor material, which limits the long-term or multiple use of the semiconductor vapour detection method. Compared to photo-stimulated semiconductor sensors, the threshold of minimum detectable concentration is lower.

A new sensor can be used for the detection of acetone vapour and its concentration. Such sensors are used, for example, for the assessment of atmospheric pollution, for the monitoring of various vapour leaks, and in the medical sector.

The minimum detectable concentration of acetone vapour is 79 times smaller (in terms of sensing area) compared to photo-stimulated semiconductor sensors currently available on the market.

The method can be used, for example, to assess atmospheric pollution, to monitor leaks of various vapours/gases, in the medical sector to analyse patients' breath to detect and evaluate possible gastrointestinal diseases, or to assess the metabolism of cells in the body, etc.

## 6.2. Procedure for the use of the acetone vapour concentration method

The measurement of the increase in the photogenerated current of the sensor output shall be used to determine the concentration of acetone vapour. A new sensor allows the detection of a minimum concentration of acetone vapour in air of 0.636 ppm (relative to a sensing area of 1 mm<sup>2</sup>) with an uncertainty of 2.0 % (95 % confidence probability) using the following operating mode parameters: HgXe lamp;  $\Phi = 4.65 \text{ mW/cm}^2$ ;  $\Phi_{\text{degassing}} = 77.5 \text{ mW/cm}^2$ ;  $U = 12 \text{ V}$ ;  $\beta = 152$ ; coupling circuit – emitter repeater with common base; ambient conditions:  $t = 20 \pm 1 \text{ }^\circ\text{C}$ ,  $r = 45 \pm 5 \text{ \%}$ .

The developed method for estimating the concentration of acetone vapour is based on the measurement of  $\Delta I$ , because this parameter shows the smallest deviation when estimating the concentration of acetone vapour (see Section 5.2). In order to be able to estimate the concentration of acetone vapour using a sensor based on optically stimulated p-n transitions, the following procedure is necessary.

1. Before using the sensor, if the sensor has been stored for a long time (more than 1 week), lower it into the acetone bath for 100 s and then rinse with an acetone jet for 10 s. The cleaning procedure should be repeated 2–3 times; after the procedure wait 2 hours before performing the following points.
2. Connect the sensor electrical circuit (Fig. 6.1, right) and prepare the measuring stand (Fig. 6.1, left). To provide the sensor with supply voltage  $U = 12 \text{ V}$ , optical stimulation of the sensor

surface with intensity  $\Phi = 4.65 \text{ mW/cm}^2$  using HgXe source. The ambient parameters must be:  $t = 20 \pm 1^\circ\text{C}$ ;  $r = 45 \pm 5 \%$ .

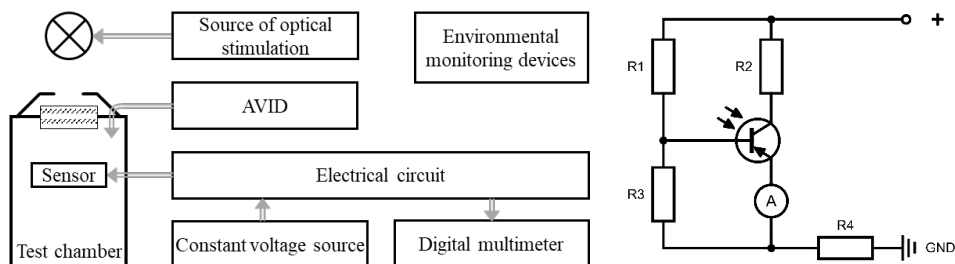


Fig. 6.1. Functional diagram of the vapour recovery device (left) and electrical circuit for the sensor (right).

Designations:  $R1=22 \text{ k}\Omega$ ;  $R2=33 \Omega$ ;  $R3=100 \text{ k}\Omega$ ;  $R4=0.11 \text{ k}\Omega$ .

### 3. Measurement procedure:

- 3.1. Sample stabilization. At this stage, the supply contacts of the electrical circuit ("+" and GND) are connected together (short circuit). 120 s after the start of the test, the sample is placed in the test chamber. 175 s after the start of the test, the power supply contacts are disconnected.
- 3.2. Switching on the power supply. At this stage, the electrical circuit is switched on for 180 seconds after the start of the test.
- 3.3. Optical surface degassing (hereinafter – degassing). The degassing stage is performed for 60 s at the optical stimulation intensity  $\Phi_{\text{degassing}} = 77.5 \text{ mW/cm}^2$ . An HgXe lamp is used as the source of optical degassing. The lamp is switched off for the next 20 s.
- 3.4. Initiation of optical stimulation. Optical stimulation is initiated at 440 seconds after the start of the experiment.
- 3.5. Acetone vapour injection. Optical stimulation continues. Acetone vapour introduced (feed time  $t = 8 \text{ s}$ ) – occurs at 540 seconds after the start of the test.
- 3.6. Completion of research. At 720 seconds, the experiment is stopped. The source of optical stimulation is switched off, the voltage supply to the sample is switched off, the chamber is opened.
4. The measurement procedure (Step 3) is repeated four times (the first three are outside the confidence interval). For the fourth time, the current is recorded during the acetone vapour injection stage.
5. The registered raw data is processed in OriginLab OriginPro 2018 (64-bit) SR1 (version: b9.5.1.195) using the following procedure:
  - 5.1. Import of raw data of the recorded current from the data log stored in the digital multimeter to the program environment (time and values of the recorded current).

- 5.2. A graph is created from the data, the program uses the baseline subtraction function (*Peak Analyzer, Goal: Subtract Baseline*). At least 7 points are used to manually determine the baseline (*BSpline*) (*Baseline Mode: User Defined*).
- 5.3. The treated registered current is the difference between the registered current and the baseline.
- 5.4. Noise compensation of the treated current value shall be performed by a 9th order polynomial approximation constructed over a period of  $\pm 20$  s from the transition point.
6. The value of emitter  $\Delta I$  is calculated using the expression:

$$\Delta I = \frac{I(\text{ac})}{I_0} \cdot 100 \%, \quad (6.1)$$

where  $I_0$  is the raw current value before acetone vapour injection,  $\mu\text{A}$ , and  $I(\text{ac})$  is the value of the treated current at the excess point – reached after the injection of acetone,  $\mu\text{A}$ .

7. Using the sensor measurement curve, estimate the acetone vapour concentration using the calculated  $\Delta I$  value (6.1).

## **7. RECOMMENDATIONS. POSSIBILITIES OF USING THE METHOD**

It is beneficial to reduce the overall dimensions of the system. To achieve the goal, these methods were evaluated.

- The system size was reduced by replacing the HgXe lamp with an LED (similar to [26], [29]). The volume of the sensor system studied in this work was about 30 l, the volume of the recommended system is about 1.5 l.  
The maximum  $\Delta I$  was determined at  $\lambda = 367.5$  nm, moreover,  $\Delta I$  decreased with increasing wavelength of optical stimulation radiation. As the number (intensity) of incident photons of optical stimulation radiation increased,  $\Delta I$  also decreased. A decrease in  $\Delta\tau$  was observed with increasing wavelength of optical stimulation. The effect of the number of falling photons on optical stimulation radiation on  $\Delta\tau$  is not clear. The study of the effect of LED radiation was performed in a saturated acetone vapour environment, because at lower vapour concentrations (for example, 13 000 ppm) it was not possible to study  $\Delta I$  due to increased noise (recorded at current value). At optical stimulation with  $\lambda = 367.5$  nm  $\Delta I$  was lower than with the HgXe lamp with UV spectrum band, so the effective wavelength of optical stimulation was less than  $\lambda = 367.5$  nm.
- System performance under different environmental conditions was carried out, as the sensors can be deployed outside the conditions in which the studies in this thesis were carried out. The study of the effect of environmental parameters (relative humidity and ambient temperature) is important because their change affects the performance of the semiconductor sensor [29], [31]. The relative humidity of the air is proportional to the amount of water



molecules that are adsorbed on the surface of the sensor. Changes in ambient temperature affect the processes that take place in the semiconductor material, so these factors can affect the results of acetone vapour concentration determination. As the temperature increased,  $\Delta I$  increased, while  $\Delta\tau$  decreased. As the relative humidity increases,  $\Delta I$ ,  $\Delta\tau$  also increases.

- Selective sensor concept to enable the method usage in gas/vapour mixtures.

The main drawback of the semiconductor gas/vapour concentration detection method is the lack of selectivity (see Table 1.1) – the difficulty of using the sensor in mixed gas/vapour environments.

The study of the new acetone vapour concentration detection method led to the conclusion that the sensitivity of the method depends on its main operating mode parameters (see Section 6.2): optical stimulation, electric circuit current voltage, surface optical degassing, current amplification factor. A correlation between  $\Delta I$  and the dipole moment of the applied vapour was observed, leading to the conclusion that the electrophysical properties of an optically induced semiconductor depend on the dipole moment of the gas.

A solution to the selective sensor concept was proposed: to use a set of sensor elements (matrix) that provide adsorption of specific gases.

## CONCLUSIONS

1. A method for the determination of acetone vapour concentration using a novel sensor based on optical stimulation of the p-n junction has been developed.
2. A method that ensures that the output photogenerated current varies with the concentration of acetone vapour in the air has been justified.
3. The sensor is based on a substantiated method.
4. A procedure has been developed and a vapour delivery apparatus has been set up to record the sensor current depending on the concentration of acetone vapour in the air.
5. Studies have been carried out on the sensor increase in output current, mode of operation of the increase in output current time interval, and parameterisation:
  - optical stimulation mode;
  - voltage of the electrical circuit;
  - optical degassing of the surface;
  - current amplification factor.
6. Studies have been carried out on the dependence of the sensor increase in output current and the time interval of the increase in output current on the concentration of acetone vapour in air.
7. A method for the determination of acetone vapour concentration in air using the new sensor based on p-n transient optical stimulation has been achieved. A procedure for the application of the method is proposed.

8. The applicability of the method, the possibility of reducing the size of the system, the operability of the system outside standard conditions are evaluated. The concept of a selective sensor is proposed.
9. For the determination of acetone vapour concentrations in air, a method was developed with a new sensor in which the p-n junction, a bipolar germanium alloy, is optically stimulated (HgXe lamp radiation, light flux  $\Phi = 4.65 \text{ mW/cm}^2$ ).
10. The sensor operates over a concentration range of 16.3 ppm to 13 060 ppm of acetone vapour.
11. The emitter current of a p-n junction based optically stimulated sensor depends exponentially on the concentration of acetone vapour in air.
12. The threshold for detection of acetone vapour concentration of the sensor is 0.636 ppm (per  $1 \text{ mm}^2$  sensing area) using the following operating mode parameters: HgXe lamp;  $\Phi = 4.65 \text{ mW/cm}^2$ ;  $\Phi_{\text{degassing}} = 77.5 \text{ mW/cm}^2$ ;  $U = 12 \text{ V}$ ;  $\beta = 152$ ; coupling circuit – emitter repeater with common base; ambient conditions:  $t = 20 \pm 1 \text{ }^\circ\text{C}$ ;  $r = 45 \pm 5 \%$ .
13. A new method for the determination of acetone vapour concentration using a sensor based on optical stimulation of the p-n junction allows the determination of a minimum concentration of acetone vapour in air of 0.636 ppm (relative to a sensing area of  $1 \text{ mm}^2$ ) with an uncertainty of 2.0 % (95 % confidence probability).

## BIBLIOGRAPHY

1. Thalakkotur, L. M., Prabhahari, P., Sukhanazerin, A., Biji, P. Technologies for Clinical Diagnosis Using Expired Human Breath Analysis. *Diagnostics (Basel)*, 2015, 5(1), 27–60. Available from: doi:10.3390/diagnostics5010027.
2. de Zwart, L. L., Meerman, J. H. N., Commandeur, J. N. M., Vermeulen, N. P. E. Biomarkers of free radical damage: Applications in experimental animals and in humans. *Free Radical Biology and Medicine*, 1999, 26(1–2), 202–226. ISSN 0891-5849. Available from: doi:10.1016/S0891-5849(98)00196-8.
3. Wang, C., Sahay, P. Breath analysis using laser spectroscopic techniques: breath biomarkers, spectral fingerprints, and detection limits. *Sensors (Basel)*, 2009, 9(10), 8230–8262. Available from: doi:10.3390/s91008230.
4. Wang, Z., Wang, C. Is breath acetone a biomarker of diabetes? A historical review on breath acetone measurements. *Journal of Breath Research*, 2013, 7(3), 1–18. Available from: doi:10.1088/1752-7155/7/3/037109.
5. Jones, A. P. Indoor air quality and health. *Atmospheric Environment*, 1999, 33(28), 4535–4564. ISSN 1352-2310. Available from: doi:10.1016/S1352-2310(99)00272-1.
6. Potyrailo, R. A., Surman, C., Nagraj, N., Burns, A. Materials and Transducers Toward Selective Wireless Gas Sensing. *Chemical Reviews*, 2011, 111(11), 7315–7354. Available from: doi:10.1021/cr2000477.
7. RAE Systems Inc. *The PID Handbook: Theory and Applications of Direct-Reading Photoionization Detectors*. Third edition. San Jose: RAE Systems by Honeywell, 2013. 167 pp. ISBN 0-9768162-1-0.
8. Korotcenkov, G. Metal oxides for solid-state gas sensors: What determines our choice? *Materials Science and Engineering: B*, 2007, 139(1), 1–23. ISSN 0921-5107. Available from: doi:10.1016/j.mseb.2007.01.044.
9. Ishihara, T., Matsubara, S. Capacitive Type Gas Sensors. *Journal of Electroceramics*, 1998, 2, 215–228. Available from: doi:10.1023/A:1009970405804.
10. Capone, S., Forleo, A., Francioso, L., Rella, R., Siciliano, P., Spadavecchia, J., Presicce, D. S. Taurino, A. M. Solid State Gas Sensors: State of the Art and Future Activities. *ChemInform*, 2004, 35. Available from: doi:10.1002/chin.200429283.
11. Mürtz, M. Breath Diagnostics Using Laser Spectroscopy. *Optics & Photonics News*, 2005, 16(1), 30–35. Available from: doi:10.1364/OPN.16.1.000030.
12. Moseley, P. T. Solid state gas sensors. *Measurement Science and Technology*, 1997, 8, 223–237. Available from: doi:10.1088/0957-0233/8/3/003.
13. Arshak, K., Moore, E., ÓLaughin, G., Harris, J., Clifford, S. A Review of Gas Sensors Employed in Electronic Nose Applications. *Sensor Review*, 2004, 24(2), 181–198. Available from: doi:10.1108/02602280410525977.
14. Liu, X., Cheng, S., Liu, H., Hu, S., Zhang, D., Ning, H. A Survey on Gas Sensing Technology. *Sensors (Basel)*, 2012, 12(7), 9635–9665. Available from: doi:10.3390/s120709635.

15. Bonch-Bruevich, V. L., Kalashnikov, S. G. *Fizika poluprovodnikov*. Moskva: Nauka, 1977. 672 p.
16. Moskatov, E. A. *Spravochnik po poluprovodnikovym priboram*. Izdanie 2. Taganrog. 219 p.
17. Stepanenko, I. P. *Osnovy teorii tranzistorov i tranzistornykh skhem*. Izdanie 4. Moskva: Energiya, 1977. 672 p.
18. Gershunskij, B. S. *Osnovy elektroniki i mikroelektroniki*. Izdanie 3. Kiev: Vishcha shkola, 1987. 422 p.
19. Wright, R. S. *EPA Traceability Protocol for Assay and Certification of Gaseous Calibration Standards*. Research Triangle Park: EPA, 2012. 174 p.
20. Hori H., Tanaka I. Equilibrated Vapor Concentrations for Bicomponent Organic Solvents. *Journal of Occupational Health*, 1998, 40(2), 132–136. Available from: doi:10.1539/joh.40.132.
21. Boumphrey, S., Marshall, N. Understanding vaporizers. *Continuing Education in Anaesthesia Critical Care & Pain*, 2011, 11(6), 199–203. ISSN 1743-1816. Available from: doi:10.1093/bjaceaccp/mkr040.
22. Green, D. W., Perry, R. H. *Perry's Chemical Engineers' Handbook*. Eighth Edition. New York: McGraw-Hill, 2008. 2700 p. ISBN 978-0-07-159313-7.
23. Poling, B. E., Prausnitz, J. M., O'Connell J. P. *Properties of Gases and Liquids*. Fifth Edition. New York: McGraw-Hill, 2001. 768 p. ISBN 978-0-07-149999-6.
24. Chou, J. *Hazardous Gas Monitors: A Practical Guide to Selection, Operation and Applications*. New York: McGraw-Hill, 2000. 258 p. ISBN 978-0-071358-76-7.
25. Dekhtyar, Y., Komars, M., Sneiders, M., Selutina, M. Towards Optically Induced Semiconductor Gas Sensor: Sensing of Acetone. *IFMBE Proceedings*, 2015, 50, 63–65. Available from: doi:10.1007/978-981-287-573-0.
26. Dekhtyar, Y., Komars, M., Sneiders, M. Optical Metrology of Novel Optically Stimulated Semiconductor Gas Sensor. *IFMBE Proceedings*, 2020, 76, 462–468. Available from: doi:10.1007/978-3-030-31635-8.
27. Dekhtyar, Y., Komars, M., Morozovs, F., Sneiders, M. Optically Induced Semiconductor Gas Sensor: Acetone Detection Range using Continuous and Cyclic Optical Irradiation Types. *IFMBE Proceedings*, 2018, 65, 330–333. Available from: doi:10.1007/978-981-10-5122-7.
28. Dekhtyar, Y., Selutina, M., Sneiders, M., Zunda, U. Towards Optically Induced Semiconductor Human Exhalation Gas Sensor. *IFMBE Proceedings*, 2016, 57, 482–485. Available from: doi:10.1007/978-3-319-32703-7.
29. Dekhtyar, Y., Komars, M., Sneiders, M. Semiconductor Ethanol Sensor Inducted with Visible Light. *IFMBE Proceedings*, 2019, 68/3, 3–6. Available from: doi:10.1007/978-981-10-9023-3.
30. Fang, F., Futter, J., Markwitz, A., Kennedy, J. UV and Humidity Sensing Properties of ZnO Nanorods Prepared by the arc Discharge Method. *Nanotechnology*, 2009, 20(24). Available from: doi:10.1088/0957-4484/20/24/245502.
31. Qiu, X., Tang, R., Zhu, J., Oiler, J., Yu, C., Wang, Z., Yu, H. The effects of temperature, relative humidity and reducing gases on the ultraviolet response of ZnO based film bulk acoustic-wave resonator. *Sensors and Actuators B: Chemical*, 2011, 151(2), 360–364. ISSN 0925-4005. Available from: doi:10.1016/j.snb.2010.07.052.